Earth and Planetary Science Letters 394 (2014) 198–208

Contents lists available at ScienceDirect

Earth and Planetary Science Letters

www.elsevier.com/locate/epsl

Distinct roles of the Southern Ocean and North Atlantic in the deglacial atmospheric radiocarbon decline

Mathis P. Hain [a,b,*], Daniel M. Sigman [a], Gerald H. Haug [c]

[a] Princeton University, Department of Geosciences, Guyot Hall, Princeton, NJ 08544, USA
[b] National Oceanography Centre Southampton, University of Southampton, SO14 3ZH, UK
[c] ETH Zürich, Geological Institute, Department of Earth Sciences, Sonneggstrasse 5, Zürich 8092, Switzerland

ARTICLE INFO

Article history:
Received 20 May 2013
Received in revised form 5 March 2014
Accepted 10 March 2014
Available online 3 April 2014
Editor: J. Lynch-Stieglitz

Keywords:
deglaciation
ice age
carbon cycle
radiocarbon
ocean circulation
AMOC

ABSTRACT

In the context of the atmospheric CO_2 $^{14}C/C$ ($\Delta^{14}C_{atm}$) changes since the last ice age, two episodes of sharp $\Delta^{14}C_{atm}$ decline have been related to either the venting of deeply sequestered low-^{14}C CO_2 through the Southern Ocean surface or the abrupt onset of North Atlantic Deep Water (NADW) formation. In model simulations using an improved reconstruction of ^{14}C production, Atlantic circulation change and Southern Ocean CO_2 release both contribute to the overall deglacial $\Delta^{14}C_{atm}$ decline, but only the onset of NADW can reproduce the sharp $\Delta^{14}C_{atm}$ declines. To fully simulate $\Delta^{14}C_{atm}$ data requires an additional process that immediately precedes the onsets of NADW. We hypothesize that these "early" $\Delta^{14}C_{atm}$ declines record the thickening of the ocean's thermocline in response to reconstructed transient shutdown of NADW and/or changes in the southern hemisphere westerly winds. Such thermocline thickening may have played a role in triggering the NADW onsets.

1. Introduction

Atmospheric $^{14}C/C$ has declined from the Last Glacial Maximum (LGM) to the preindustrial modern, with two main episodes of rapid $\Delta^{14}C_{atm}$ decline during deglaciation (e.g., Hughen et al., 2004; Bronk Ramsey et al., 2012; Southon et al., 2012) (Fig. 1). The significance of this record is vigorously debated. Two explanations have been proposed for the sharpest $\Delta^{14}C_{atm}$ declines: (a) the Southern Ocean ventilation of an hypothesized isolated volume of carbon dioxide-rich abyssal water, yielding synchronous atmospheric CO_2 rise and $\Delta^{14}C_{atm}$ decline (Broecker and Barker, 2007; Marchitto et al., 2007; Skinner et al., 2010), or (b) the resumption of NADW formation transferring ^{14}C from the atmosphere into the deep ocean (Keir, 1983; Hughen et al., 1998, 2004; Köhler et al., 2006; Laj et al., 2004; Muscheler et al., 2008), in which case $\Delta^{14}C_{atm}$ is expected to decline most steeply only after most of the atmospheric CO_2 rise. In general, however, skepticism has been expressed that any oceanic mechanism can explain the observed $\Delta^{14}C_{atm}$ changes (Broecker, 2009).

Here, supported by an improved estimate of ^{14}C production rate change, we attempt a complete simulation of the deglacial $\Delta^{14}C_{atm}$ history. We find that the $\Delta^{14}C_{atm}$ history is surprisingly consistent with the consensus view of deglacial ocean changes, with alternating increases in North Atlantic deep ventilation and Southern Ocean CO_2 release. Two subtle but coherent deviations between model and observations that immediately precede the onsets of NADW formation at ~12 and ~15 thousand years before present (kyr BP) can be taken as evidence for one further ingredient, and we will argue that this as-of-yet unrecognized dynamic may be important in the mechanism of the South-to-North teleconnection.

2. Methods

2.1. The new CYCLOPS model

All carbon cycle model simulations in this study were generated using a new high-performance implementation of the legacy CYCLOPS global carbon cycle box model (e.g., Hain et al., 2010; Keir, 1988; Sigman et al., 1998, 2003; Robinson et al., 2005b). We use the same model configuration as in (Hain et al., 2010, 2011), with 18 ocean reservoirs, one atmospheric carbon reservoir, and one fixed size terrestrial carbon reservoir (3000 PgC). The operation of the biological carbon pumps is simulated as in (Hain et al., 2010). The lysocline model controlling the open system $CaCO_3$ cycle is a combination of the "rain-based" version of seafloor $CaCO_3$ model of (Sigman et al., 1998), the bottom water under-saturation driven part of the (Archer, 1991) $CaCO_3$ diagenesis model, and net-throughput sediment mixed layer model with

* Corresponding author at: National Oceanography Centre Southampton, University of Southampton, SO14 3ZH, UK.
E-mail address: m.p.hain@soton.ac.uk (M.P. Hain).

http://dx.doi.org/10.1016/j.epsl.2014.03.020
0012-821X/

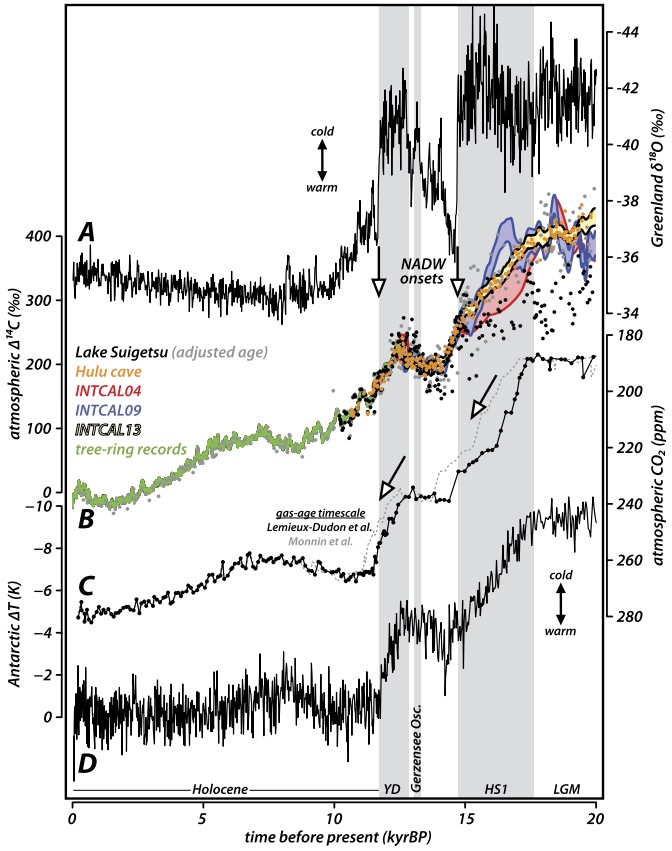

Fig. 1. Records of deglacial changes in climate and the carbon cycle. (A) Greenland (NGRIP) ice core $\delta^{18}O$ on GICC timescale (Andersen et al., 2006; NGRIP members, 2004; Rasmussen et al., 2006; Vinther et al., 2006). (B) Atmospheric $\Delta^{14}C$ ($\Delta^{14}C_{atm}$) datasets (Bronk Ramsey et al., 2012; Southon et al., 2012; Reimer et al., 2009, 2004, 2013). (C) Reconstructed atmospheric CO_2 levels (gray dashed: Monnin et al., 2001) on revised timescale (black: Lemieux-Dudon et al., 2010). (D) Antarctic temperature changes (Jouzel et al., 2007). The driving mechanisms for rapid $\Delta^{14}C_{atm}$ decline ~12 and ~15 kyrs BP are debated, with ocean CO_2 release and North Atlantic circulation changes as the main contending explanations.

millennial adjustment timescale for percent $CaCO_3$ on the seafloor (see Supplementary Information).

2.2. Sensitivity experiments

In this study, we consider the effect of six distinct mechanisms that are linked to deglacial changes in ocean circulation and biogeochemistry (reviewed by Hain et al., 2014): (#1) Polar Antarctic stratification during the LGM, with subsequent destratification (e.g., François et al., 1997; Sigman et al., 2010); (#2) glacial expansion and deglacial retreat of Southern Ocean sea ice (e.g., Collins et al., 2012; Stephens and Keeling, 2000); (#3) the deglacial rise of Polar Antarctic preformed nutrient concentration (François et al., 1997; Robinson et al., 2004; Robinson and Sigman, 2008); (#4) the rapid end of enhanced iron fertilization in the Subantarctic (Kohfeld et al., 2005; Kumar et al., 1995; Martin, 1990; Martinez-Garcia et al., 2009) that led to a rise in surface nutrient concentration (Robinson et al., 2005b; Martinez-Garcia et al., 2014); (#5) the stalling of Atlantic meridional overturning associated with Heinrich Stadial 1 (HS1) and the Younger Dryas (YD) (e.g., Lippold et al., 2012; McManus et al., 2004; Robinson et al., 2005a); and (#6) the abrupt resumption of North Atlantic Deep Water formation at the onsets of the Bølling/Allerød interstadial and the Holocene interglacial (e.g., McManus et al., 2004; Ritz et al., 2013; Robinson et al., 2005a). Additionally, we test for the impact of deepening/thickening of the ocean's main thermocline, which we will argue below caused $\Delta^{14}C_{atm}$ decline just prior to NADW resumption at the end of HS1 and YD.

All transient sensitivity experiments are initialized with the steady state LGM carbon cycle scenario of (Hain et al., 2010, 2011), to which we have increased sea ice cover in the Antarctic, reducing the surface area available for gas-exchange of the Polar Antarctic Zone (PAZ) box by 50%. From this starting point, individual Southern Ocean-related model parameters (#1–4) were abruptly reverted to their respective interglacial model reference values. For the North Atlantic circulation changes, we test both the abrupt transition from GNAIW-circulation to (#5) HS-circulation and to (#6) NADW-circulation (Fig. S1). All individual sensitivity experiments and their outcomes are described in detail in the Supplementary Information and listed in Table S1 for 1, 5 and 60 thousand years after the abrupt forcing. For brevity, Section 3.1 describes only the 1 kyr sensitivities and conflates the Polar Antarctic Zone experiments (#1–3).

The use of "GNAIW" circulation for the LGM (instead of the IG reference "NADW" circulation) directly relates to the finding of a mid-depth Atlantic $\delta^{13}C$ gradient during the LGM, which implies shoaling of the depth to which the ice age North Atlantic ventilated the ocean interior (e.g., Duplessy et al., 1988; Curry and Oppo, 2005; Marchitto and Broecker, 2006; see review by Lynch-Stieglitz et al., 2007). It also relates to the very high $\delta^{13}C$ and low nutrient concentration of northern-sourced water during the LGM (Marchitto et al., 1998), the combination of which is difficult to simulate without allowing the downstream advection of North Atlantic-sourced mid-depth water to extend beyond the Atlantic basin (Sigman et al., 2003). We note that, in the GNAIW circulation scheme (Sigman et al., 2003), wind-driven upwelling in the open Antarctic returns mid-depth water (instead of deep water, as in the NADW scheme) to the surface so as to balance the formation of intermediate-depth rather than deep water in the North Atlantic (Fig. S1).

2.3. ^{14}C production and global budget

The global budget of ^{14}C and the abundance of ^{14}C on the planet during the deglaciation are a function of the time-variant rate of cosmogenic ^{14}C production and the regular radioactive decay of this isotope (with a half-life of 5730 yr). Cosmogenic ^{14}C production is affected by the strength of Earth's magnetic field, which shields the atmosphere from high energy cosmic particles, and the solar modulation of the incidence of high energy cosmic particles (Lal and Peters, 1967).

To calculate the global budget of ^{14}C, we extend and update the approach of Hughen et al. (2004), Köhler et al. (2006) and Laj et al. (2002, 2004):

(1) The GLOPIS-75 reconstruction of Earth's magnetic field strength of the last 75 thousand years ago and the associated uncertainty envelope (Laj et al., 2004) are used with linear interpolation (Fig. 2A).
(2) Using a recent model of cosmogenic production of ^{14}C (Kovaltsov et al., 2012), global ^{14}C production (Fig. 2B) is calculated as a function of the time-variant GLOPIS-75 field strength (M) and a constant solar modulation potential (Φ = 550 MV; see also Bard, 1998). Using the Kovaltsov et al. (2012) model, we calculate a modern ^{14}C production rate of ~1.8 atom cm^{-2} s^{-1} (Fig. 2B), a preindustrial bulk global decay rate of ~1.7 dps cm^{-2} (Fig. 2C), and a global bulk $\Delta^{14}C$ of −110‰ (Fig. 2D), which is in good agreement with the $\Delta^{14}C$ of the ocean carbon pool. As pointed out by Kovaltsov et al. (2012), earlier models (e.g., 2.05 atom cm^{-2} s^{-1}, Masarik and Beer, 2009) overestimated global ^{14}C production due to outdated cosmic ray spectra used in the calculations.